Synthesis and Polyelectrolyte Behavior of Poly(methacrylic acid) Star Polymers

Taiichi Furukawa, Satoshi Uchida, Koji Ishizu

Department of Organic Materials and Macromolecules, International Research Center of Polymer Science, Tokyo Institute of Technology, Ookayama, Meguro-ku, Tokyo 152-8552, Japan

Received 10 March 2006; accepted 12 June 2006
DOI 10.1002/app.24966
Published online 25 April 2007 in Wiley InterScience (www.interscience.wiley.com).

ABSTRACT: Poly(*tert*-butyl methacrylate) [P(*t*BMA)] star polymers were synthesized by copolymerization of p(*t*BMA) macroinitiator with ethylene glycol dimethacrylate via atom transfer radical polymerization method. P(*t*BMA) stars had a narrow molecular weight distribution (M_w/M_n = 1.06–1.15). The ratio of radius of gyration to hydrodynamic radius R_G/R_H, which indicates inner segment density, was in the range 1.16–1.22 in tetrahydrofuran (THF) (arm number f = 25–142). These stars behaved not as hard spheres but as soft spheres in THF. Poly(methacrylic acid) stars were obtained by the hydrolysis of P(*t*BMA) arms. We investigated the conformation of star polyelectrolyte as a function of pH and ionic strength by means of dynamic light scattering (DLS). The hydrodynamic diameter increased gradually from 18.8 to 48.3 nm as a function of the solution pH. In addition, we compared experimental results with theoretical models for star polyelectrolytes. © 2007 Wiley Periodicals, Inc. J Appl Polym Sci 105: 1543–1550, 2007

Key words: ATRP; soft sphere; star polyelectrolyte

INTRODUCTION

Star-branched polymers are characterized as structures, where all the chains of a molecule are linked together to a small-molar-mass core. Generally, star polymers exhibit smaller hydrodynamic dimensions than the linear polymer with identical molar mass. The interest in star polymers arises not only from the fact that they are models for branched polymers but also from their enhanced segment densities. Zimm and Stockmayer were the first to study the conformation of star-branched polymers using classical theories.[1] Daoud and Cotton studied the conformation and dimensions of star polymers using scaling theories.[2] Recently, we synthesized polyisoprene (PI) stars by copolymerization of PI-lithium with divinylbenzene (DVB) in heptane. The conformation of these star molecules in good solvents was in agreement with the Daoud–Cotton scaling model of stars. Their solution properties suggested that they behaved not as hard spheres but as soft spheres.[3]

Stars with multiarms (the critical number of arms is estimated to be of order 10^2) are expected to form a crystalline array near the overlap threshold (C^*) by Witten et al.[4] We investigated in detail the structural ordering of stars by means of small-angle X-ray scattering (SAXS).[5] PI stars (arm number $f \gg \sim 90$) formed a body-centered-cubic (bcc) structure near C^*. This structure changed to a mixed lattice of bcc and face-center-cubic (fcc) structures with increasing polymer concentration. We also synthesized functionalized poly(ethylene oxide) (PEO) stars possessing a tertiary amino group at each arm end. Subsequently, positive charges were introduced into such peripheral tertiary amino groups by quaternization with methyl iodide (CH_3I). It was found that these peripherally charged stars ($f \gg 37$) formed a lattice of bcc below C^* due to electrostatic repulsion between stars.[6] There has been rapid growth in the area of controlled/living radical polymerization: atom transfer radical polymerization (ATRP),[7,8] nitroxide-mediated radical polymerization,[9] and reversible addition-fragmentation chain-transfer polymerization (RAFT)[10] have been widely employed for preparing star-shaped polymers. There are also some recent reports concerning the preparation of star polymers with living polymerization strategies.[11–15]

Polyelectrolytes are polymer chains containing ionizable groups. Solution properties of these polymers are different from those of uncharged polymers due to dissociation of ionizable groups. Experimental and theoretical studies on the conformation of star polyelectrolytes in solution have been enough undertaken. Recently, the conformation and interactions of star-branched polyelectrolytes have also been studied in some details, using light,[16] neutron,[17] X-ray scattering,[18] scaling theory,[19] and computer simulations.[20] However, only a few works have reported the behavior of star polyelectrolytes from an experimental point

Correspondence to: K. Ishizu (kishizu@polymer.titech.ac.jp).

Journal of Applied Polymer Science, Vol. 105, 1543–1550 (2007)

of view. Heinrich et al.[21] and Moinard et al.[18] investigated the solution properties (structural ordering) of sodium sulfonated polystyrene (PSSNa) stars and poly (sodium acrylate) (PANa) stars using SAXS. In these works, the arm numbers of stars were small. Reports of the studies concerning the stars with multiarms have apparently not been published to date.

In this article, we present the synthesis of P(*t*BMA) star polymers with various arm number or Poly (methacrylic acid) [P(MAA)] star polymers. We also investigated the conformation of star polyelectrolytes as a function of pH and ionic strength by means of dynamic light scattering (DLS). In addition, we compared experimental results with theoretical models for star polyelectrolytes.

EXPERIMENTAL

Materials

tert-Butyl methacrylate (*t*BMA) and ethylene glycol dimethacrylate (EGDMA) (Tokyo Kasei, Tokyo) were distilled in high vacuum. Tetrahydrofuran (THF), toluene, 1,4-dioxane, methanol, methyl 2-bromopropionate (Tokyo Kasei, Tokyo), ultrapure water, HCl, NaOH (Kanto Kagaku, Tokyo), CuCl (Wako Pure Chemical Industries, Tokyo), and *N*,*N*,*N*′,*N*″,*N*″-pentamethyldiethylenetriamine (PMDETA) (Aldrich, Milwaukee, WI) were used as received.

Synthesis and characterization of P(*t*BMA) macroinitiators

P(*t*BMA) macroinitiators were synthesized using CuCl complexed by PMDETA as the catalyst and methyl 2-bromopropionate as the initiator in THF at 60°C. P(*t*BMA) macroinitiator was precipitated in methanol/H_2O (7/3 v/v) after passing through an alumina column to remove the copper complexes. The number-average molecular weight (M_n) and the molecular weight distribution (M_w/M_n) were determined by gel permeation chromatography (GPC; Tosoh high-speed liquid chromatography HLC-8020), which was operated with TSK gel G2000H_{XL} (excluded-limit molecular weight $M_{EL} = 1 \times 10^4$) and two GMH_{XL} columns ($M_{EL} = 4 \times 10^8$), in series using THF as the eluent (flow rate 1.0 mL/min) at 40°C.

Synthesis of P(*t*BMA) stars

P(*t*BMA) stars were synthesized by copolymerization of P(*t*BMA) macroinitiator with EGDMA with CuCl complexed by PMDETA as the catalyst in toluene (200 mL) at 80°C. After the polymerization, the reaction solvent was changed to THF after removing toluene using a rotary evaporator and was precipitated in methanol/H_2O (7/3 v/v) after passing through an alumina column to remove the copper complexes. Unreacted P(*t*BMA) was removed from the polymerization products by the precipitation fractionation with a THF-methanol/H_2O system.

A combination of GPC with light scattering (LS) detector is very useful for measuring the weight-average molecular weight (M_w) of branched polymers such as star polymers, since one does not need any isolation procedures to remove unreacted arm polymers. GPC measurements were carried out with a Tosoh high-speed liquid chromatography HLC-8120 equipped with a low-angle laser light scattering (LALLS) detector (LS-8: He–Ne laser with a detection angle of 5°) and refractive index (RI), which was operated with TSK gel G2000H_{XL} and two GMH_{XL} columns (in series) using THF as the eluent at 40°C. The conversion of star polymers was determined by the ratio of the peak of the P(*t*BMA) star to the total peak area of the polymerization product in GPC charts. The details concerning the calculation method have been given elsewhere.[22]

Hydrolysis of P(*t*BMA) stars

P(*t*BMA) stars were derived into poly(methacrylic acid) [P(MAA)] stars by the hydrolysis of P(*t*BMA) arms. Concentrated HCl was added to the solution of P(*t*BMA) star polymer in 1,4-dioxane, and the solution was heated to reflux for 6 h at 90°C. The reaction solution was cooled, and the excess reagents were removed under vacuum. The disappearance of *t*BMA units was confirmed by ^1H nuclear magnetic resonance (NMR; 500 MHz, JEOL GSX-500 NMR spectrometer) in CD_3OD.

Dilute-solution properties of stars

The M_w of the fractionated P(*t*BMA) stars was determined by static light scattering (SLS; Photal TMLS-6000HL: Otsuka Electronics, $\lambda_0 = 632.8$ nm) in THF at 25°C in Zimm mode. The scattering angle was in the range 30°–150°. The RI increment dn/dc (= 0.04 mL/g in THF) of p(*t*BMA) star polymer was measured with a differential refractometer (Photal DRM-1021: Otsuka Electronics). Sample solutions were filtered through membrane filters with a nominal pore of 0.2 μm just before measurement.

The diffusion coefficient (D_0) of P(*t*BMA) stars was determined by the extrapolation to zero concentration on dynamic light scattering (DLS: Otsuka Electronics) data with cumulant method at 25°C in THF. The scattering angle was 90°.

The hydrodynamic radius (R_H) of P(MAA) stars was determined by CONTIN method on DLS at 25°C in NaOH aqueous solution.

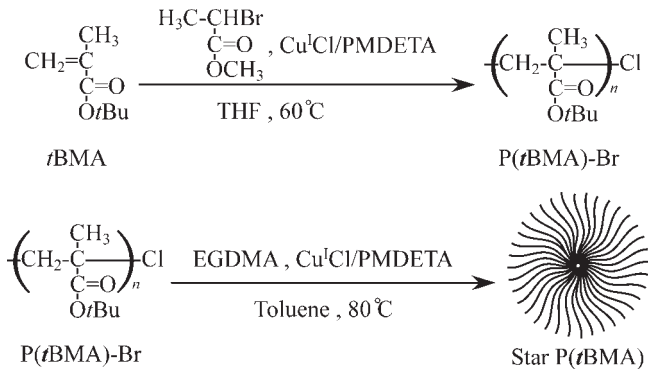

Scheme 1

RESULTS AND DISCUSSION

Synthesis of P(*t*BMA) stars

Controlled/''living'' radical polymerization processes have proven to be versatile for the synthesis of polymers with well-defined structures. We synthesized star polymers by ATRP method. The synthetic route of P(*t*BMA) stars is shown in Scheme 1. According to the experimental procedure, CuCl was used as a catalyst with methyl 2-bromopropionate as the initiator. Because of the halide exchange equilibrium and the relative strengths of carbon-halogen bonds, the majority of the polymer chains should in fact contain Cl end groups.[23,24] A typical GPC profile of P(*t*BMA) (BMA1) is shown in Figure 1. The GPC profile of BMA1 shows unimodal pattern and relatively narrow molecular weight distribution ($M_w/M_n = 1.14$).

Subsequently, we synthesized P(*t*BMA) star polymers with various arm numbers by varying the feed ratio [EGDMA]/[M] ([M] is the feed concentration of macroinitiator). To set up higher polymerization temperature, the solvent was changed from THF to toluene. Table I lists polymerization conditions and results for P(*t*BMA) stars. In no case were crosslinked or insoluble materials observed. Copolymerization of P(*t*BMA) macroinitiator with EGDMA seemed to proceed within miceller domains, because the copolymerization behavior in which crosslinked or insoluble materials have never been observed. In the initial stage, P(*t*BMA) macroinitiator is consumed rapidly with EGDMA. Therefore, part of the feed P(*t*BMA) macroinitiator would form linear P(*t*BMA)-*block*-poly(EGDMA). Toluene may be somewhat poor solvent for poly (EGDMA) chains. This is uncertain problem in this work. Figure 1 also shows typical GPC profile of polymerization product SBMA1, using RI and LS detectors. The GPC distribution has a bimodal pattern. The first peak at lower elution volume in RI chart corresponds to the P(*t*BMA) star polymer. The GPC elution pattern of the second peak is identical with that of BMA1. Then, polymerization product SBMA1 is a mixture of P(*t*BMA) star and unreacted P(*t*BMA) homopolymer. The conversion of star polymer was 61%. However, this conversion was lower than that

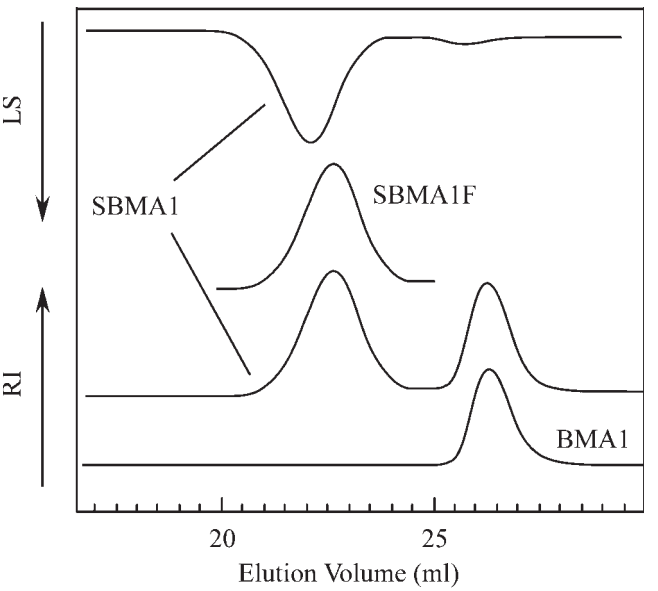

Figure 1 GPC profiles of P(*t*BMA) star SBMA1, star fraction SBMA1F, and P(*t*BMA) homopolymer BMA1.

TABLE I
Reaction Conditions and Results of P(*t*BMA) Stars

	Feed conditions		Arm		Star		
Sample	[M] (mmol/L)	[EGDMA]/[M] (mol/mol)	M_w[a] (10^{-4})	M_w/M_n[a]	M_w[b] (10^{-6})	M_w/M_n[c]	Conversion (%)
SBMA1	22.0	15	1.4	1.14	1.2	1.13	61
SBMA2	22.1	10	1.1	1.07	0.7	1.06	51
SBMA3	22.1	20	2.0	1.26	2.8	1.15	46
SBMA4	22.2	5	1.4	1.31	0.5	1.12	49
SBMA5	22.2	7	1.1	1.21	0.3	1.14	71

All reactions were carried out with [Macroinitiator]:[CuCl]:[PMDETA] = 1 : 1.1 : 1.1, under high vacuum at 80°C in toluene for 72 h.

[a] Determined by GPC using universal calibration.

[b] Determined by SLS in THF.

[c] Determined by GPC equipped with LS detector.

reported by Matyjaszewski and coworkers in reports by ATRP,[25,26] which reached 80–90%. It is well known for the block copolymer synthesis that poly(methacrylate) macroinitiator having a bromine atom at the end group effectively initiated the ATRP of methacrylate monomers in the presence of the catalyst CuCl; that is, halide exchange should take place.[27–29] Halide exchange contributes to increase the relative rate of initiation to propagation. To achieve high conversion for the star synthesis, we will need to use such halide exchange equilibrium.

Figure 2 shows the plots of the arm number or M_w/M_n against the feed ratio [EGDMA]/[M] ([M] = 2.2×10^{-2} mol/L). The arm number increases gradually with an increase of [EGDMA]/[M]. The polydispersity is relatively narrow ($M_w/M_n = 1.06$–1.15). Therefore, it was found that the arm number was controlled by varying the feed ratio [EGDMA]/[M]. Each star (BMA-F) was removed from the corresponding unreacted P(*t*BMA) homopolymer by the precipitation fractionation with a THF-methanol/water system (see Fig. 1).

Dilute-solution properties of P(*t*BMA) stars

To investigate the behavior of P(*t*BMA) stars in dilute solution, we examined the dilute solution properties using DLS in THF at 25°C. The observed physical values of P(*t*BMA) stars are listed in Table II. Figure 3 shows the relationship between translational diffusion coefficient $D(C)$ and polymer concentration C for SBMA1F and SBMA2F. Each $D(C)$ has an almost constant value. The values of D_0 for SBMA1F and SBMA2F were 1.5×10^{-7} and 2.0×10^{-7} cm^2/s, respectively. This suggests that these P(*t*BMA) stars form a single molecule in THF. Similar tendencies were also observed in $(AB)_n$ star block,[30] prototype,[31] and double-cylinder type copolymer brushes.[32] The translational diffusion coefficient, D_0 can be estimated by extrapolation of polymer concentration to zero. The hydrodynamic radius (R_H) can be estimated by the Stokes–Einstein's equation $R_H = kT/6\pi\eta_0 D_0$, where k, T, and η_0 indicate Boltzmann coefficient, absolute temperature, and viscosity of solvent, respectively. In early report,[33] we judged the shape of polystyrene stars in the solid state through transmission electron microscopy (TEM). It was found from that micrograph that isolated stars showed spherical shape in the solid state. P(*t*BMA) stars seem to be spherical in THF as well.

TABLE II
Characteristics of P(*t*BMA) Stars

Sample	M_w[a] (10^{-6})	M_w/M_n[b]	Arm number	R_G[a] (nm)	R_H[c] (nm)	R_G/R_H
SBMA1F	1.2	1.13	90	16.3	13.6	1.20
SBMA2F	0.7	1.06	60	12.5	10.3	1.22
SBMA3F	2.8	1.15	142	17.6	15.2	1.16
SBMA4F	0.5	1.12	34	13.1	10.8	1.21
SBMA5F	0.3	1.14	25	12.5	10.2	1.22

[a] Determined by SLS in THF.
[b] Determined by GPC using universal calibration.
[c] Determined by DLS in THF.

The ratio R_G/R_H is a sensitive fingerprint of the inner density profile of star molecules and polymer micelles. The values of R_G/R_H for P(*t*BMA) stars were in the range of 1.16–1.22 (arm number $f = 25$–142). It is well known that R_G/R_H for unperturbed polymers

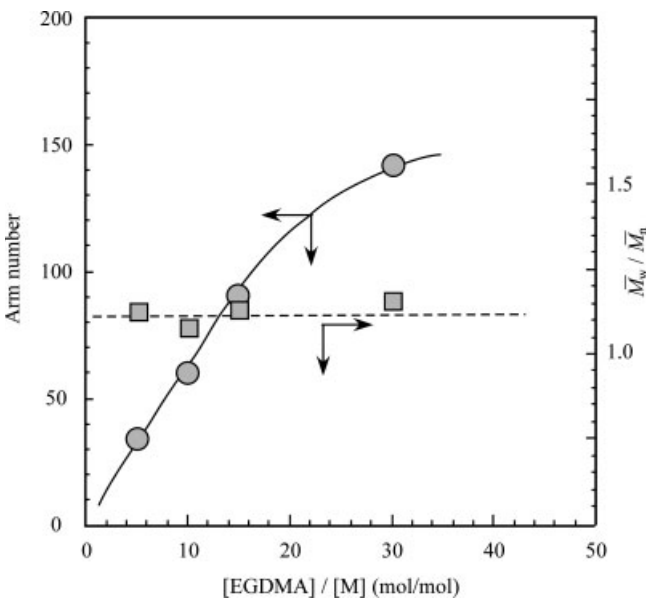

Figure 2 Plots of the arm number or polydispersity against the feed ratio [EGDMA]/[M] ([M] = 2.2×10^{-2} mol/L).

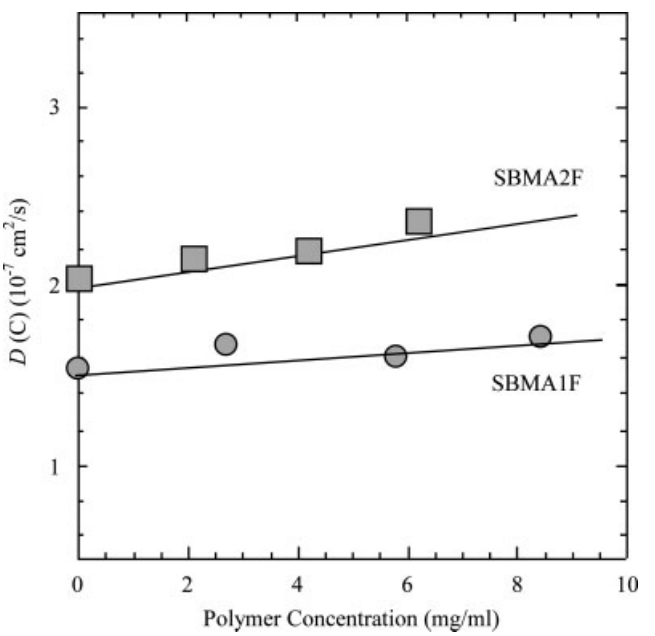

Figure 3 Plots of translational diffusion coefficient $D(C)$ of P(*t*BMA) stars (SBMA1F and SBMA2F) as a function of polymer concentration.

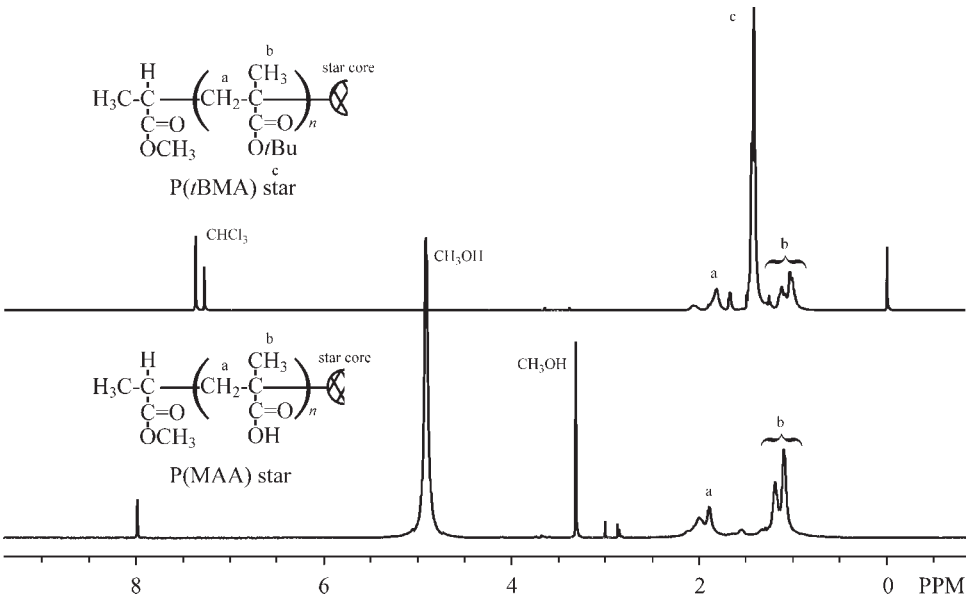

Figure 4 ^{1}H NMR spectra of (a) P(*t*BMA) star (SBMA5F) and (b) P(MAA) star (SMAA5F).

and hard spheres with uniform density are 1.25–1.37[34] and 0.775,[35] respectively. Recently, we prepared DVB core-crosslinked PI stars ($40 < f < 237$). The values of R_G/R_H in cyclohexane decreased gradually and approached unity as f became large.[3] In fact, the R_G/R_H for SBMA3F composed of higher arm number ($f = 142$) was of smaller value ($R_G/R_H = 1.16$). It was concluded that the stars with multiarm behaved not as hard spheres but as soft spheres that were penetrable near the edge in a good solvent. The results obtained in this work showed the same behavior.

Dilute-solution properties of P(MAA) Stars

The *tert*-butyl ester groups were hydrolyzed using excess HCl in refluxing 1,4-dioxane for 6 h. Figure 4(a) shows ^{1}H NMR spectrum of the original P(*t*BMA) stars in $CDCl_3$. This spectrum shows the resonance for the methylene protons (a; δ 1.8 ppm), the methyl protons (b; δ 1.0 and 1.1 ppm) of main chain, and the *tert*-butyl protons (c; δ 1.4 ppm). ^{1}H NMR spectrum of P(MAA) star polymer in CD_3OD shows the disappearance of the *tert*-butyl groups at δ = 1.4 ppm [see Fig. 4(b)]. There are peaks that are not identified in both spectra. They are due to impurities. The hydrolysis was seemed to proceed almost perfectly.

In recent years, Borisov and Zhulina[19] describe the conformation of weak star-branched polyelectrolytes in dilute solution and the dependence of the overall star size on the number of branches on the ionic strength of solution. Thus, we examined the dilute solution properties of P(MAA) star polymers using DLS in aqueous solution. It is well known that DLS data for linear polyelectrolyte shows multimodal size distribution due to inhomogeneous distribution of counterions. However, for branched polyelectrolyte such as stars, most of the counterions are trapped inside the stars, while the concentration of counterions in the interstar regions is considerably smaller than the average value. This can be shown by direct measurement of the osmotic pressure of the counterions of salt-free solutions of the spherical polyelectrolyte brushes by Das et al.[36] Groenewegen et al. have also reported the counterions distribution in the coronal layer of polyelectrolyte diblock copolymer micelles by means of SANS experiments.[37] They concluded that all counterions were trapped in the coronal layer. Figure 5 shows the plots of the translational diffusion coefficient $D(C)$ as a function of the polymer concentration [Fig. 5(a)] and the size distribution for SMAA5F [Fig. 5(b)]. This constant value of $D(C)$ and unimodal size distribution for P(MAA) star suggest that most of the counterions are trapped inside the stars and the polyelectrolyte effect of interchain interactions can be ignored. Hence, the measured D_H derived from the diffusion coefficient directly reflects the polymer architecture.

For a weak polyelectrolyte such as our case, two different classes exist. When the fractional charge is very small, the electrostatic screening length is much larger than the overall star size, and hence, inside the star there is no screening of Coulomb interaction. With increasing of the fractional charge, the majority of the counterions are trapped within the arm, and now, the concomitant osmotic pressure gives the main contribution to the arm stretching force. The crossover between the unscreened and the screened osmotic stars occurs at $f \cong f^*$ where[38]

$$f^* \cong \alpha^{-1/2}(l_B/a)^{-1} \quad (1)$$

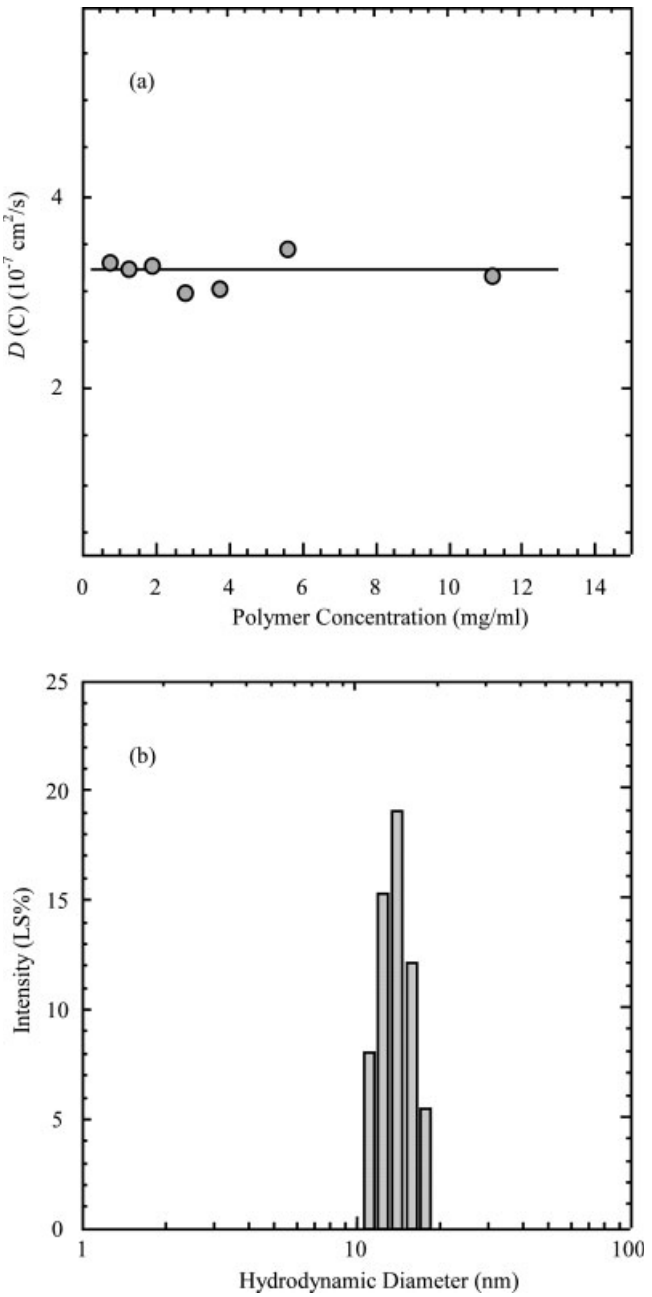

Figure 5 (a) Plot of translational diffusion coefficient $D(C)$ as a function of the polymer concentration for SMAA5F and (b) size distribution for SMAA5F.

with α the fraction of charged monomer, l_B the Bjerrum length (0.7 nm at 298K), and a the monomer unit length. For stars with multiarms, the unscreened regime can only be observed for $\alpha \ll 1$. Because of $f \gg 20$, all of our samples are in the osmotic regime. The D_H increases gradually due to the concomitant arm chain expansion from 18.3 to 48.3 nm. This chain expansion originates from the osmotic pressure exerted by the counterions trapped within the arm chain. The chain extension, which means the degree of chain expansion, is estimated from the D_H and the contour length of the P(MAA) unit (89 monomer units per arm chain with a vinylic step length of 0.252 nm). As a result, the P(MAA) chains take gradually a stretched structure from 0.37 to 0.98, which indicates an almost fully stretched configuration at high pH and no added salt.

Consequently, the measured D_H dependence on α is compared to the prediction by theoretical models to gain additional insight concerning the charged nature. The fraction of dissociation α of the carboxyl groups can be calculated from the solution pH and the dissociation constant pK_a by

$$\mathrm{pH} = pK_a + \log\frac{\alpha}{1-\alpha} \tag{2}$$

The value of pK_a was determined to be 6.6 for SMAA5F from the titration curve. The double-logarithmic plot of D_H as a function of α is shown in Figure 6. It is found that the D_H is proportional to the 0.39th power of the fraction of dissociation α. Borisov and Zhulina[19] have presented the model for weak polyelectrolyte star in salt-free solution. For osmotic stars, their model describes the overall star size $L \sim \alpha^{1-\nu}N$, where N indicates the monomer unit of arm. Here, ν is equal to 1/2 or 3/5 for the system without chain volume interactions or with such interactions, respectively. The experimental data indicate $\nu = 3/5$ and agree very well with good solvent system.

In general, ionic charges do not dissociate and condense in the presence of inorganic salt. We investigated the dependence of the overall star size on the

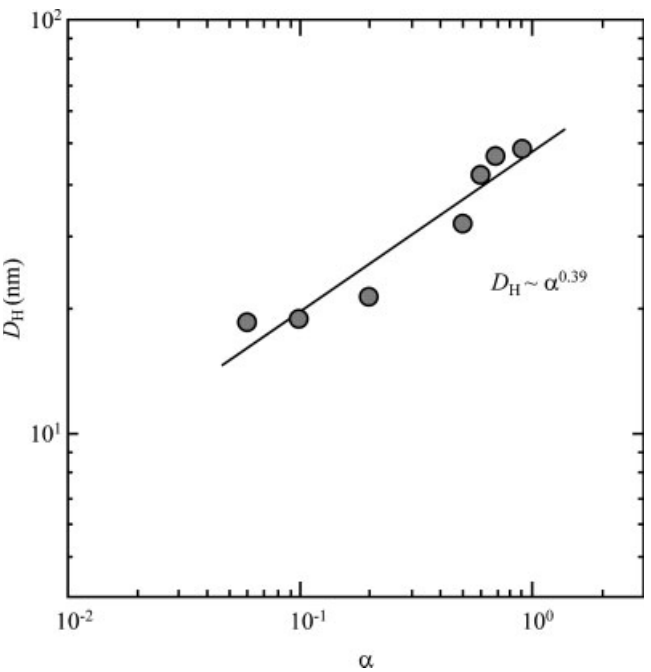

Figure 6 Plot of D_H as a function of degree of dissociation α for P(MAA) star.

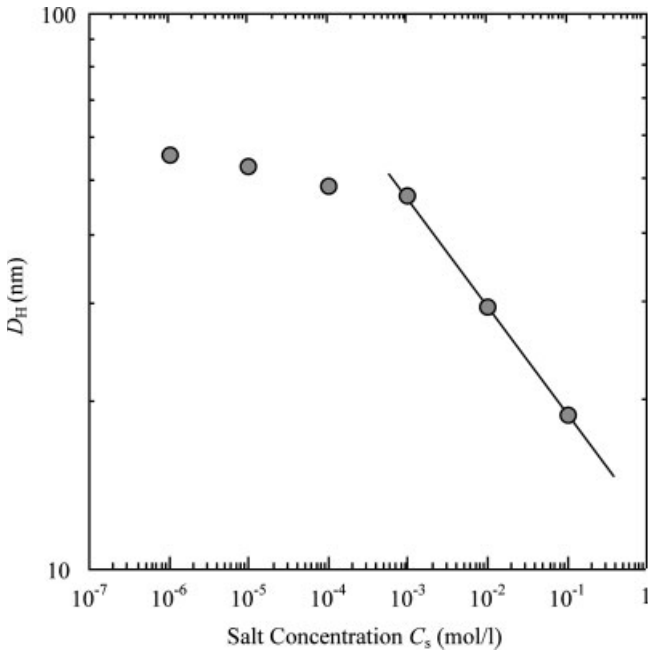

Figure 7 Double-logarithmic plot of hydrodynamic diameter D_H as a function of salt concentration C_S.

ionic strength of solution with the addition NaCl. Figure 7 shows the double-logarithmic plot of the D_H as the function of the salt concentration C_s. The D_H levels off with decreasing salt concentration. On the other hand, the D_H is proportional to the –0.19$_7$th power of the salt concentration in excess of 1×10^{-3} mol/L. As mentioned above, the intramolecular Coulombic repulsion in many-armed stars is already partially screened in the salt-free solution by counterions localized preferentially in the intrastar space. Hence, the high salt concentration requires affecting the conformation of the star. In other words, the salt concentration in the bulk of the solution must exceed significantly the intrinsic concentration of counterions to affect the star conformation. Thus, at small salt concentration, the overall star size shrinks gradually from 55.4 to 48.8 nm because the intramolecular screening is dominated by counterions, while in the limit of high salt ($C_s \gg 1 \times 10^{-3}$ mol/L), both coions and counterions contribute significantly to the screening of the intrastar Coulombic repulsion, resulting in the steeper shrinkage of the star size. The size of the star in the salt-dominance regime predicted by Borisov and Zhulina[19] is given by

$$L \cong N^{3/5} f^{1/5} \alpha^{2/5} C_s{}^{1/5} \quad (3)$$

The close agreement with their theory indicates that in the limit of high salt ($C_s \gg 1 \times 10^{-3}$ mol/L), the concentration of counterions inside the star is the same as that of coions in bulk solution. In this work, we studied the solution properties using one star sample SMAA5F. This star exhibits the smallest arm length (degree of polymerization = 77) and the lowest arm number ($f = 25$) in the samples prepared. Then, such polyelectrolyte behaviors may appear strongly for other star samples, because other samples possess more compact and larger particle conformations.

CONCLUSIONS

P(*t*BMA) star polymer was synthesized by copolymerization of P(*t*BMA) macroinitiator with EGDMA via ATRP method. P(*t*BMA) stars had a narrow molecular weight distribution. The arm number was controlled by varying the feed ratio [EGDMA]/[M]. It was concluded from the results of SLS and DLS that these stars behave not as near hard spheres but as soft spheres in THF. P(MAA) stars were obtained by the hydrolysis of P(*t*BMA) arms. The structure of these stars in dilute aqueous solution was investigated as a function of pH, α, and ionic strength. At full ionization, the arm chains are almost fully stretched with a density scaling proportional from the core. These behaviors agreed well with the theoretical models. These results were strikingly different from the situation for uncharged spherical polymers and star polymers, where the chains take a more compact coiled structure.

References

1. Zimm, B. H.; Stockmayer, W. H. J Chem Phys 1949, 17, 1301.
2. Daoud, M.; Cotton, J. P. J Phys (Paris) 1982, 43, 531.
3. Ishizu, K.; Ono, T.; Uchida, S. Macromol Chem Phys 1997, 198, 3255.
4. Witten, T. A.; Pincus, P. A.; Catea, M. A. Europhys Lett 1986, 2, 137.
5. Ishizu, K.; Ono, T.; Uchida, S. J Colloid Interface Sci 1997, 192, 189.
6. Furukawa, T.; Ishizu, K. Macromolecules 2003, 36, 434.
7. Matyjaszewski, K.; Xia, J. Chem Rev 2001, 101, 2921.
8. Kamigaito, M.; Ando, T.; Sawamoto, M. Chem Rev 2001, 101, 3689.
9. Hawker, C. J.; Bosman, A. W.; Harth, E. Chem Rev 2001, 101, 3661.
10. Chiefari, J.; Rizzardo, E. In Handbook of Radical Polymerization; Matyjaszewski, K.; Davis, T.P., Eds.; Wiley-Interscience: New York, 2002; p 629.
11. Du, J.; Chen, Y. J Polym Sci Part A: Polym Chem 2004, 42, 2263.
12. Deng, M.; Chen, X.; Piao, L.; Zhang, X.; Dai, Z.; Jing, X. J Polym Sci Part A: Polym Chem 2004, 42, 950.
13. Gaillard, N.; Guyot, A.; Claverie, J. J Polym Sci Part A: Polym Chem 2003, 41, 2567.
14. Zhou, H.; Jiang, J.; Zhang, K. J Polym Sci Part A: Polym Chem 2005, 43, 2567.
15. Reddy, S. K.; Sebra, R. P.; Anseth, K. S.; Bowman, C. N. J Polym Sci Part A: Polym Chem 2005, 43, 2134.
16. Sedlak, M. Langmuir 1999, 15, 4045.
17. Boue, F.; Cotton, J. P.; Lapp, A.; Jannink, G. J Chem Phys 1994, 101, 2562.
18. Moinard, D.; Taton, D.; Gnanou, Y.; Rochas, C.; Borsali, R. Macromol Chem Phys 2003, 204, 89.

19. Borisov, O. V.; Zhulina, E. B. Eur Phys J B 1998, 4, 205.
20. Roger, M.; Guenoun, P.; Muller, F.; Belloni, L.; Delsanti, M. Eur Phys J E 2002, 9, 313.
21. Heinrich, M.; Rawiso, M.; Zilliox, J. G.; Lesieur, P.; Simon, J. P. Eur Phys J E 2001, 4, 131.
22. Ishizu, K.; Shimomura, K.; Saito, R.; Fukutomi, T. J Polym Sci Part A: Polym Chem 1991, 29, 607.
23. Matyjaszewski, K.; Shipp, D. A.; Wang, J. L.; Grimaud, T.; Patten, T. E. Macromolecules 1998, 31, 6836.
24. Haddleton, M.; Heming, A. M.; Kukulj, D. Chem Commun 1998, 1719
25. Xia, J.; Zhang, X.; Matyjaszewski, K. Macromolecules 1999, 32, 4482.
26. Zhang, X.; Xia, J.; Matyjaszewski, K. Macromolecules 2000, 33, 2340.
27. Shipp, D. A.; Wang, J. L.; Matyjaszewski, K. Macromolecules 1998, 31, 8005.
28. Chatterjee, D. P.; Mandal, B. M. Polymer 2006, 47, 1812.
29. Karanam, S.; Gossens, H.; Klumperman, B.; Lemstra, P. Macromolecules 2003, 36, 3051.
30. Ishizu, K.; Uchida, S. Prog Polym Sci 1999, 24, 1439.
31. Tsubaki, K.; Kobayashi, H.; Satoh, J.; Ishizu, K. J Colloid Interface Sci 2001, 241, 275.
32. Tsubaki, K.; Ishizu, K. Polymer 2001, 42, 8287.
33. Ishizu, K.; Ono, T.; Uchida, S. Polym Plast Technol Eng 1997, 36, 461.
34. Roovers, J; Martin, J. E. J Polym Sci Part B: Polym Phys 1989, 27, 2513.
35. Antonietti, M.; Gremser, W.; Schmidt, M. Macromolecules 1990, 23, 3796.
36. Das, B.; Guo, X.; Ballauff, M. Prog Colloid Polym Sci 2002, 121, 34.
37. Groenewegen, W.; Lapp, A.; Egelhaaf, S. U.; van der Maarel, J. R. C. Macromolecules 2000, 33, 4080.
38. Hariharan, R.; Biver, C.; Russel, W. B. Macromolecules 1998, 31, 7514.